VOL. 11, NO. 23, DECEMBER 2016 ISSN 1819-6608
ARPN Journal of Engineering and Applied Sciences

www.arpnjournals.com

DEVELOPMENT OF A FORCE FEEDBACK SYSTEM FOR A SCORBOT ROBOTIC ARM GRIPPER

Praneel Chand[1], Sunil Lal[2] and Rahul Kumer[3]
[1]Department of Vehicle Systems and Materials/ Department of Engineering, Unitec Institute of Technology, Auckland, New Zealand
[3]School of Engineering and Advanced Technology, Massey University, New Zealand
[3]School of Engineering, the University of the South Pacific, Fiji
E-Mail: pchand3@unitec.ac.nz

ABSTRACT

This paper presents the development of a linear control based force feedback system for a scorbot robotic arm. The scorboter-4u is a 5 degree of freedom (DOF) robotic arm with a 2-fingered parallel configuration gripper. A flexi-force force sensitive Resistor (FSR) is attached to one of the claws of the gripper and interfaced to a laptop computer controllerviaan Arduino Uno microcontroller. The force sensor assists the robot in three different ways. Firstly, it provides feedback on a successful grasping task. Secondly, through iterative experiments, the coefficient of friction of the object being manipulated can be determined. Thirdly, force control on the target object being manipulated can be established to prevent damage. The gripper and force sensor combination is calibrated prior to grasping objects. MATLAB 2014a is used to command both the scorbot er-4u's control box and Arduino Uno force sensor controller.

Keywords: robotic arm, gripper, force feedback, calibration, control, force sensor.

1. INTRODUCTION

For robotic arms, the end - effector is an indispensable component which physically interacts with the environment. They are commonly used for painting, welding, drilling and also for pick and place tasks. Additionally, they are used for medical applications [1-3] as well. In many cases handling of the target object is critical. To some extent, the design of the end of the arm tooling (which is the tool attached to the end effector), is task oriented making it quite expensive and time consuming. Many efforts have been made to eliminate the human operator for three major reasons[4]: to save labour costs, to reduce product damage (when it comes to handling for products or the semiconductor devices) and to improve human safety (handling of radioactive or corrosive components). When interacting with a target object, it is inevitable that some amount of force is exerted onto the object. This force must be controlled to finish the task successfully without product damage.

Controlling the force exerted on an object during grasping is easily implemented by the human hand. Its capability to apply just the right amount of force is likely to be unmatched in comparison with artificial prosthetic hands. However, researchers have strived to come closer in developing technologies which would mimic a human arm. To understand the concept of grasping, enthusiasts have studied the human arm which is said to have a total of 22 degrees of freedom [5].

An approach is taken in [6] to mathematically model the thumb and a finger of human subjects to generate position profiles with varying speed of finger movement. In the study, a force sensor was used to measure the bending angle of the human finger while performing a gripping like action. In [7], through tactile sensing, a Willow Garage PR2 robot was used to perform an object grasping task where the developed controller generates tactile signals to prevent slippage of the object. Moreover, [8] presented Bayesian inference and biologically inspired algorithms for the control of tangential forces on an anthropomorphic mechatronic prosthetic hand. The Kalman filter is applied to the biomimetic tactile sensor data to filter out noise for the calculation of the tangential force. In [9], focus was done on strengthening an anthropomorphic robot hand to make it capable of exerting a large grasping force upon grasping an object. Additionally, in [10], the anthropomorphic robotic arm is used to manipulate remote objects through teleoperation. The user manipulates the object through the linkage with a control rig. The force incurred in the robotic arm (which is used to interact with the object remotely) is fed back to the user.

In [11], a force imaging approach is utilised to tackle the problem of grasping and manipulation through demonstration. By deploying an image sensor (camera), a Fanuc robot is taught by a human how to grasp, pick and place an object. The Fanuc robot was able to mimic what the human teacher demonstrated to it. In addition to this, [12]developed a 16 × 16 FSR to recognize small sized 3D objects with the use of machine learning techniques. Whilst being a reliable and cheap solution for rough visualization of the 3D objects, this method was limited to relatively large and solid objects.

Inspired from the biological configuration of the human arm, in most of applications 2-fingered [13] or 3-fingered [14] grippers are used to facilitate similar tasks[2, 7-12]. In [13], a 2-fingered flexible gripper with a force sensor attachment employs a proportional integral control method to grasp objects. The control scheme for the system is simple. However, it's modelling is complex despite being able to manipulate rigid and flexible objects.

From the surveyed literature it can be said that an FSR is a versatile transducer to utilise when it comes to force analysis and force sensitive applications. Hence, this paper proposes using the Tekscan's Flexi - Force[15] FSR to measure the gripping force on arigid 2-fingered parallel configuration gripper of the 5 DOF scorbot er-4u robotic

arm[16]. This particular model of the scorbot does not incorporate a force feedback system from the manufacturer. Using the Tekscan FSR provides a simple and low cost solution for the force feedback system. The robotic arm is currently being refurbished and redesigned for use as a part sorting robot. At the high level control, the platform incorporates an intelligent vision system for object detection and recognition [17] and a multi-layered feed-forward artificial neural network based kinematics algorithm [4] as a solution to inverse kinematics.

A conceptual diagram of the force feedback system is illustrated in Figure-1. The remainder of this paper focuses on development, testing and evaluation of the scorbot robotic arm force feedback system.

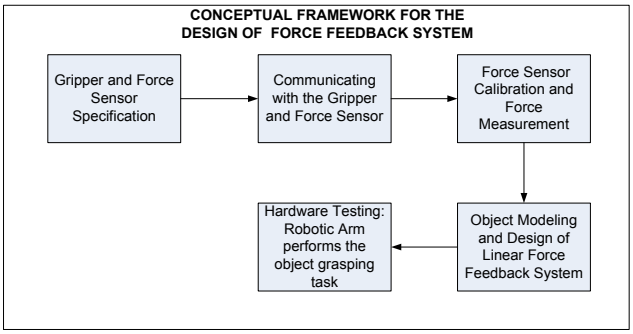

Figure-1. Conceptual framework for the design of the force feedback system.

2. GRIPPER AND FORCE SENSOR SPECIFICATIONS

A. The Gripper

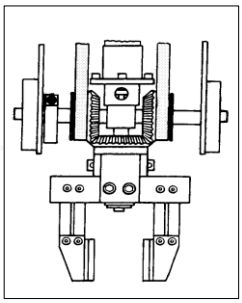

Figure-2. SCORBOT ER-4u's Gripper.

The gripper as shown in Figure-2 is the end effector of the robot which is attached to the wrist of the scorbot er-4u. The gearing mechanisms enable it to open and close depending on user requirements. This gripper mimics human fingers (thumb and pointer) capable of holding, tightening and releasing an object. It has a maximum payload of 2kg and is driven by a 12V DC servo motor whose position feedback is provided by incremental optical encoders. The gripper can open up to 75mm (without rubber pads) and 65mm (with rubber pads). In addition, both the fingers/claws of the gripper move simultaneously (2-Finger Parallel configuration).

B. The force sensor

Figure-3. The force sensitive resistor.

The force sensor used is a Flexi-Force FSR manufactured by Tekscan [15]. It is a 191mm long flexible force resistive sensor which is 0.203mm thick. The range of force which can be measured is 0N to 445N.However, forces out of this range can be measured via an amplification technique. For the current application, the sensing range will not exceed 445N.

3. COMMUNICATING WITH THE GRIPPER AND THE FORCE SENSOR

A. Gripper

The gripper control is achieved using MATLAB via a USB connection. Figure-4details how the connection is established.

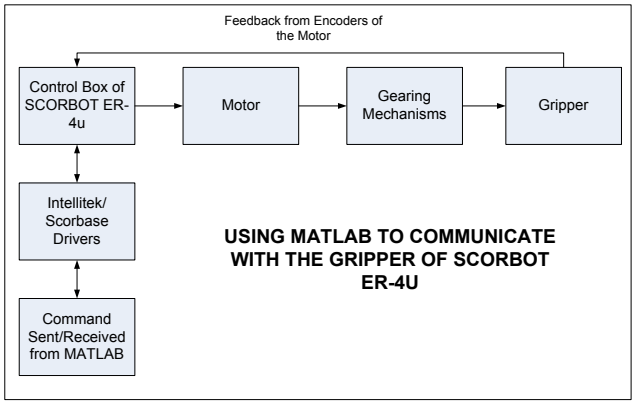

Figure-4. Communication with the Gripper through MATLAB.

From the MATLAB command prompt, motor commands are sent to the MTIS Intermediary DLL, to the Intellitek's Name mangled DLL, and then to the control box for actuation through the USB cable. The motor along with the gear mechanisms operate to produce the desired gripper positioning. The gripping range is from 0mm to 65mm (with rubber pads), hence, each gripper claw can movea maximum of 32.5mm to close the gripper.

B. Force sensor

Through the analog GPIO pins of Arduino Uno, it is possible to interface the force sensor and acquire data. However, analysis is done on MATLAB to achieve a real

time control system for the gripper. Using MATLAB's hardware support packages, a connection between Arduino Uno and MATLAB is established. This enables a single programming environment (MATLAB) to be used for control.Figure-5below shows the procedure for connecting to the force sensor to get feedback.

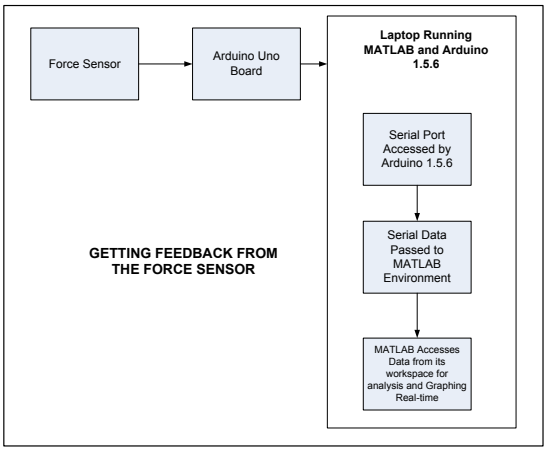

Figure-5. Getting feedback from the force sensor.

4. FORCE SENSOR CALIBRATION AND FORCE MEASUREMENT

The Flexi-Force FSR offers a repeatability of less than 2.5% along with a response time of less than 5µs[15]. The entire sensing area of the FSR is subjected to different masses for calibration. Since the FSR has a circular sensing area with a diameter of 9.53mm, a small puck with parameters equivalent to the FSR sensing area was placed before putting masses to calibrate the sensor. The mass of the small circular puck is equal to 0.00024g which is negligible in comparison with the calibration masses. The calibration process set up is shown in Figure-6.

Figure-6. FSR interfaced using Arduino Uno and MATLAB (with puck for calibration).

The FSR is attached to a Digital Measuring Scale (DMS) and a small puck is placed on top of it. The DMS is reset once the puck and the FSR are placed on it. Every time a mass is added, the reading from the DMS is used to determine the force exerted onto the FSR and the corresponding voltage representing force is read using the Arduino-Uno.

A simple voltage divider circuit was preferred over the circuit in [15]. The electrical circuit diagram for interfacing the FSR using the voltage divider circuit is illustrated in Figure-7.

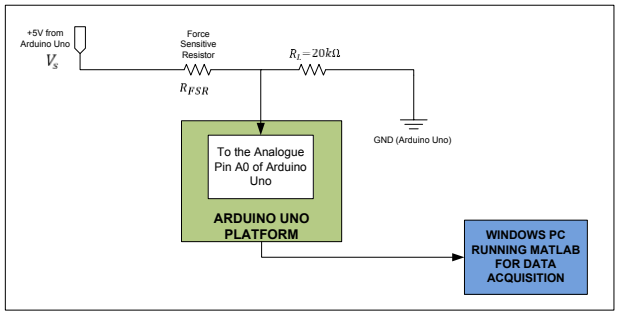

Figure-7. Interfacing FSR using Arduino Uno and MATLAB.

Using the circuit(Figure-7), the FSR is calibrated using known masses. Figure-8 shows the force sensor being calibrated using known masses. A graph is plotted in real time using MATLAB to ensure consistent force readings.

Figure-8. Calibration of force sensor in real time.

In order to convert force into volts, the following procedure is used. From Figure-7, the voltage at the analog pin A0 is:

$$V_{A0} = \frac{R_L}{R_L + R_{FSR}} \times V_S \quad (1)$$

Where V_S is 5V supplied by Arduino-Uno microcontroller. The input voltage at pin A0 isrepresented as an8-bitADC value b. Hence, the input range for $V_{A0}$is from 0 - 255 which corresponds to 0 - 5V respectively. An algorithm does this conversion upon the acquisition of voltage data using MATLAB. Equation (2) describes how the voltage incurred at pin A0 is converted from 8-bit data to a voltage:

$$V_{A0} = \frac{b}{255} \times 5 \quad (2)$$

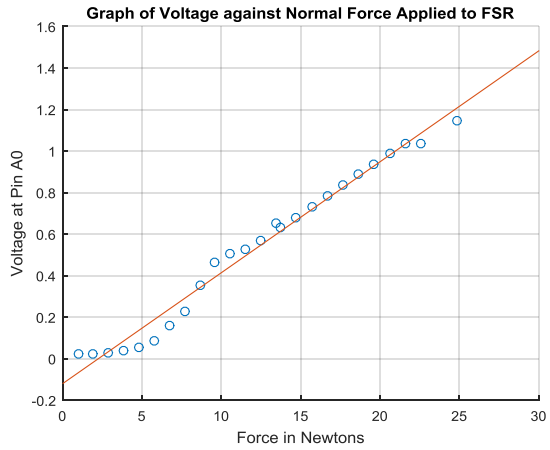

Figure-9. Graph of voltage against the normal force applied to FSR

Figure-9 shows the relationship between the voltages at pin A0 and the normal forces applied to the FSR during calibration. Using this relationship, the voltages represent how much force is directly applied onto the FSR. From Figure-9 it can be seen that:

$$V_{A0} \alpha F_N \quad (3)$$

Using the polyfit command in MATLAB [18]which is based on Vandamonde's matrix [19], a linear equation(4) is derived to represent the relationship.

$$V_{A0} = 0.0534F_N - 0.1201 \quad (4)$$

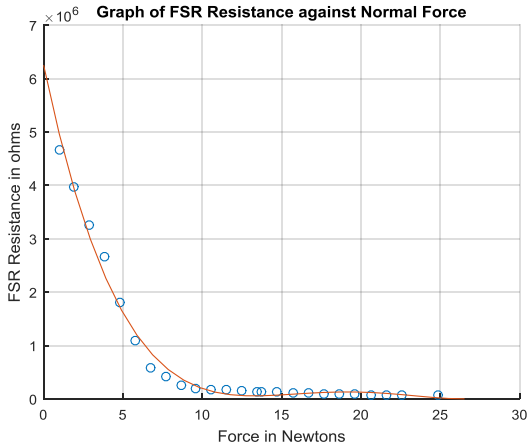

Figure-10. Graph of FSR resistance against the normal force.

Figure-10 illustrates the change in resistance of the FSR measured using a Fluke Digital Multimeter (DMM) during calibration. To obtain a linear relationship, conductance (5) is used to get Figure-11.

$$G = \frac{1}{R_{FSR}} \quad (5)$$

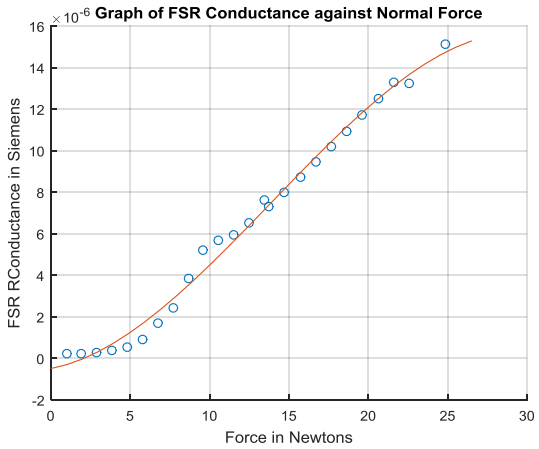

Figure-11. Graph of FSR conductance against normal force.

This step is used to verify the voltage readings taken at pin A0 (V_{A0}) of the Arduino-Uno. The linear equation for Figure-11 using the polyfit command in MATLAB is given by:

$$G = 1 \times 10^{-5}(0.0687F_N - 0.1965) \quad (6)$$

5. OBJECT MODELLING AND DEVELOPMENT OF LINEAR FORCE CONTROL

A. Object modelling

Based on the proposed task for the robotic arm [17], the objects are limited to the following characteristics:

- uniform size and shape.
- overall length or width or diameter should be less than 65mm.
- weight should not exceed 2kg. (payload of SCORBOT ER-4u)

Figure-12 shows the forces applied to the object when a rigid 2-fingered parallel configuration gripper is used for grasping.

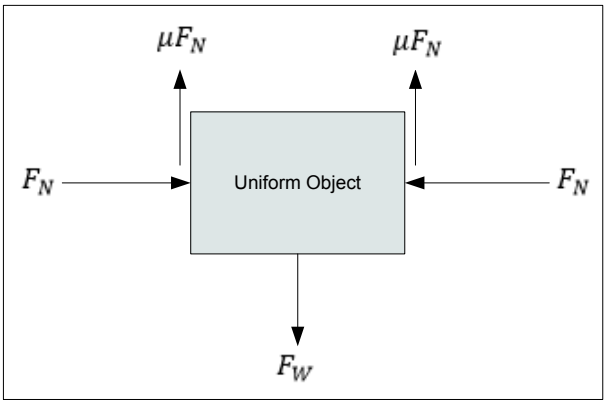

Figure-12. Applied force on the object.

The force exerted by the 2-fingered configuration gripper is identical and normal to the object, which is represented by F_N (normal force). $F_W$is the force due to the weight of the object, and μ is the coefficient of static friction of the object.

B. Relationship between weight force and sensor readings

In similar manner to the force sensor calibration (section IV), another experiment was carried out to grasp known weights (F_W) in increments of 0.1N from 0N to 2.0N using the gripper of the robotic arm. Readings were taken for successful object grasping with the application of minimum force. A set up of the experiment using the scorbot robotic arm is shown in Figure-13.

Figure-13. Normal force data logging using MATLAB.

In the same manner as section IV, the graphs of voltage, resistance and conductance are drawn as a function of weight forceF_W.

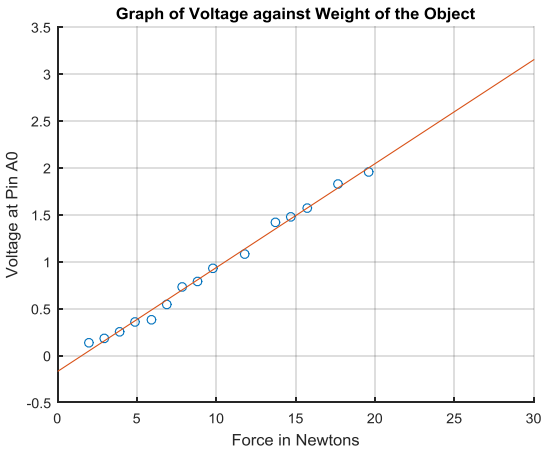

Figure-14. Graph of voltage against the weight of object.

Using the *polyfit* curve fitting algorithm in MATLAB, the linear relationship between V_{A0} and F_W in Figure-14 is given by:

$$V_{A0} = 0.1107F_W - 0.1695 \quad (7)$$

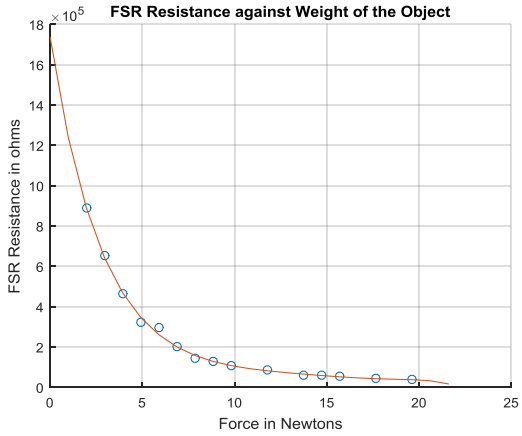

Figure-15. Graph of FSR resistance against the weight of object.

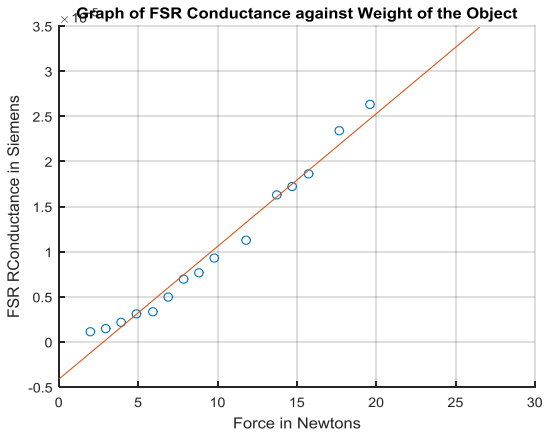

Figure-16. Graph of FSR conductance against the weight of object.

Similarly, using the definition of conductance from (5), the linear relationship between G and F_W is given by:

$$G = 1 \times 10^{-5}(0.1828F_W - 0.5106) \quad (8)$$

C. Establishing grasping force for the Gripper of SCORBOT ER-4u

In section IV, the FSR was turned into a force measuring device through calibration. Additionally, in Figure-12, the normal force F_N, is same as the grasping force incurred by the claws of the 2-fingered parallel configuration gripper. The actual normal/grasping force can be found by equating (4) and (7), as well as (6) and (8). The conductance equations are used as a comparison model to ensure correct outputs for F_N are provided from the voltage quantities. Equating (4) and (7) gives the normal/grasping force as:

$$F_N = \frac{1}{0.0534}(0.1107F_W - 0.0494) \quad (9)$$

Similarly, equating (6) and (8) gives:

$$F_N = \frac{1}{0.0632}(0.1470F_W - 0.12135) \quad (10)$$

Equations (9) and (10) represent approximately the same value of grasping force F_N which must be provided by the gripper of the robot to successfully grasp an object of weight F_W without damaging it.

6. RESULTS AND DISCUSSIONS

A. Demonstration of linear force control using Gripper of SCORBOT ER-4u

Figure-17 describes the object grasping process carried out by the gripper of the robot based on the readings from the FSR. Each reading is compared with the stored value of grasping force and the grasping will halt only if the reading from FSR is within the tolerance range of $\pm$0.1N. This is done to ensure the safety of the object. The first part is to establish linear control using the data gathered during calibration. The second is to perform object grasping using the established control and indicate successful grasping of the object.

Using the grasping force F_N as derived in section V *C*, the gripper was tested using masses with same coefficient of friction. Masses of 200g, 400g, 600g and 1200g were used to test the proposed linear force control of the gripper. The F_N required for the masses 200g, 400g, 600g and 1200 are 3.14N, 7.21N, 15.34 and 23.48N, respectively using either (9) or (10). Figures 18-21 show the real time graphs of grasping force when the gripper performs the grasping task on the respective masses. After a stable response and holding the object, the force returns to zero indicating that the gripper has released the object.

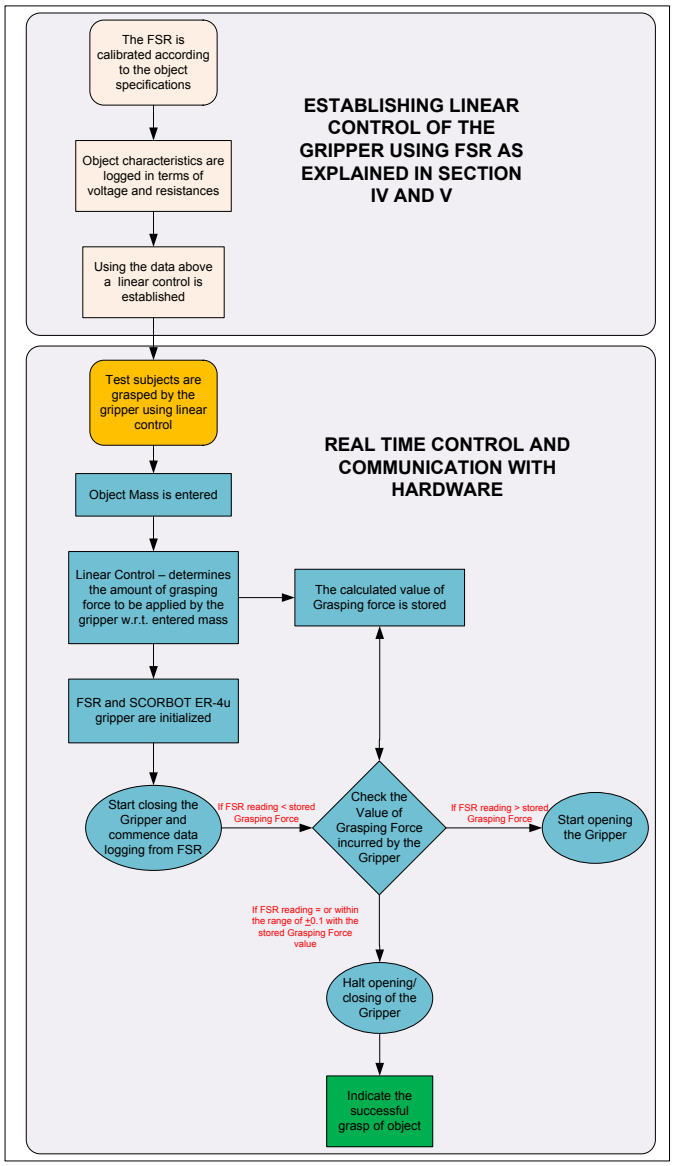

Figure-17. Object grasping program flow.

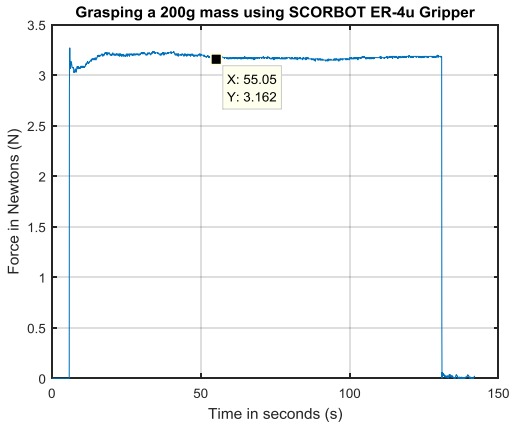

Figure-18. 200g object grasping by SCORBOT ER-4u Gripper (Hardware).

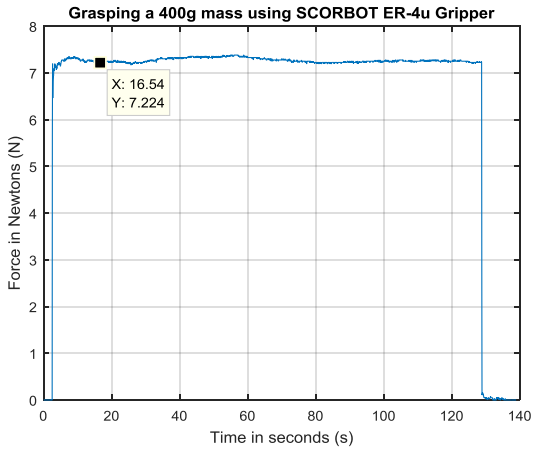

Figure-19. 400g object grasping by SCORBOT ER-4u Gripper (Hardware).

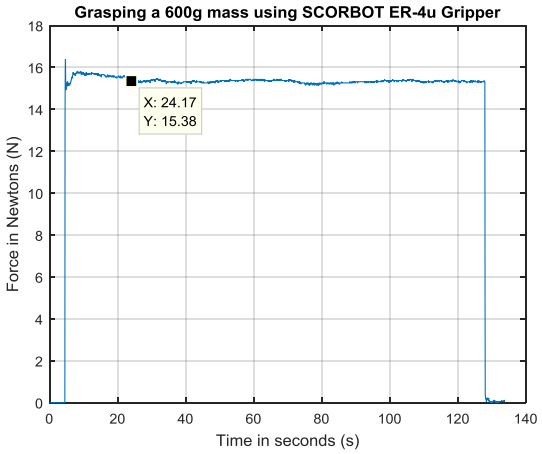

Figure-20. 600g object grasping by SCORBOT ER-4u Gripper (Hardware).

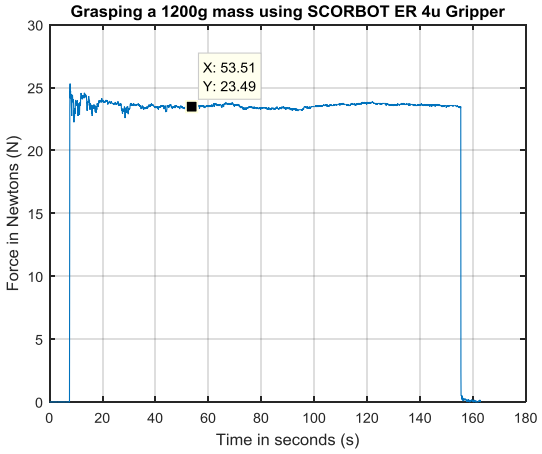

Figure-21. 1200g object grasping by SCORBOT ER-4u Gripper.

The highlighted points (x and y coordinates) in the graphs above represent the end time, for which the gripper is successfully able to grasp the object. The settling time is calculated based on the start time (Impact detection at the FSR) and end time (stable response in the graph) as shown in Table-1.

Table-1. Settling time calculation.

Figure	Start time	End time	Settling time (End time - Start time)
18	5.738	55.05	49.312
19	2.508	16.54	14.032
20	4.477	24.17	19.693
21	11.12	53.51	42.39

Using the program structure in Fig. 17, Figs. 18-21 show the status of the gripper while performing a grasping action. It can be deduced from the graphs that in order to successfully grasp an object, the applied force must be within a certain range. In Figures 18-21, the x-coordinate represents the end time and the y-coordinate represents the force applied by the gripper to successfully grasp the object. Initially, the tolerance range for the gripper was set to $\pm$0.5N.Duringhardware testing this tolerance range was reduced to $\pm$0.1N to achieve better results and safety of the object (reduce the risk of falling).

For the cases above, it can also be seen that if there is some change in the FSR reading, the gripper will try to readjust by either opening or closing the gripper.

B. Demonstration of successful grasping of the object

In addition to the linear force control, deploying the force sensor has its advantages. Through the readings of the force sensor, the status of the gripper can be easily monitored. As in the Figure 18-21, the FSR is able to convey:

a) Impact detection (when the object is being first touched by the gripper)
b) Process of grasping (when the gripper is applying sufficient amount of force to grasp the object completely according to the derived linear F_N)
c) Final stable response (constant graph after (ii) to indicate that the object is successfully grasped and there is no slippage)

C. Determining the coefficient of friction

Using the free body diagram (FBD) of the object (Figure-12), the coefficient of static friction between the rubber pad of the gripper and the object can be determined. The μ is calculated by finding slope from the graph of frictional force against the normal force. Frictional force is determined using the data obtained from calibration and also using the FBD in Figure-12. The graph below shows the plot where voltage and conductance quantities are used to find outμ.

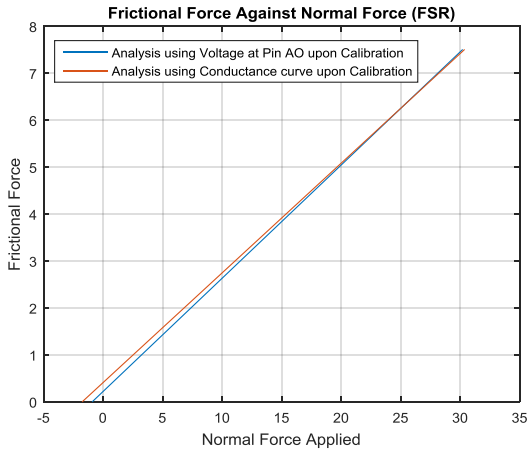

Figure-22. Frictional force against normal force.

The slight deviation is attributed to the difference in DMM and computer readings. However, the values are same within the tolerance range. The relationship between frictional force and normal force using voltage and conductance quantities respectively are:

$$F_{R(VOLTAGE)} = 0.2412F_N + 0.2231 \quad (11)$$

$$F_{R(CONDUCTANCE)} = 0.2387F_N + 0.4128 \quad (12)$$

From the gradients of (11) and (12), the coefficient of static friction μ, betweenthe rubber pad of the gripper and the object is approximately 0.24.

7. CONCLUSIONS

This paper has presented the development of a linear force feedback system for the gripper of the scorbot er-4u robotic arm. The gripper did not previously have a force feedback system and this feature has now been added as part of the robot's refurbishment. The force sensor was attached to a 2-fingered parallel configuration gripper of scorbot er-4u and a linear relationship was derived between the normal/grasping force and weight of the object. A linear control for grasping force was established as a function of weight of the object.

Hardware tests were carried out to evaluate the system. The force sensor successfully indicated on the status of the grasped object. Using the developed linear force control method,the objects were handledproperlyby applying adequate amount of force without damaging the object. However, this was limited to objects which had approximately the same coefficient of friction (determined from the calibration stage). It was also noted from the results that a large settling time is required to achieve a successful grasp of an object.

Future work will include approaches to optimize and build a more intelligent control for this robotic arm. To grasp objects with unknown masses or coefficient of friction a vision system can be integrated with the force control.

ACKNOWLEDGEMENT

The authors would like to thank the Technicians of the School of Engineering at USP for their assistance in carrying out hardware experiments.

REFERENCES

[1] E. Dégoulange, L. Urbain, P. Caron, S. Boudet, J. Gariépy, J.-L. Megnien, *et al.* 1998. HIPPOCRATE: an intrinsically safe robot for medical applications. in Intelligent Robots and Systems, 1998. Proceedings, 1998 IEEE/RSJ International Conference on. pp. 959-964.

[2] F. Pierrot, E. Dombre, E. Dégoulange, L. Urbain, P. Caron, S. Boudet, *et al.* 1999. Hippocrate: a safe robot arm for medical applications with force feedback. Medical Image Analysis. 3: 285-300.

[3] W. S. Ng. 1998. Articulated arm for medical procedures. ed: Google Patents.

[4] R. R. Kumar and P. Chand. 2015. Inverse kinematics solution for trajectory tracking using artificial neural networks for SCORBOT ER-4u. in Automation, Robotics and Applications (ICARA), 2015 6th International Conference on. pp. 364-369.

[5] C. Toledo, L. Leija, R. Munoz and A. Vera. 2009. Upper limb prostheses for amputations above elbow: A review. in Health Care Exchanges, 2009. PAHCE 2009. Pan American. pp. 104-108.

[6] M. M. Rahman, T. T. Choudhury, S. N. i. Sidek and A. Awang. 2014. Mathematical Modeling and Trajectory Planning of Hand Finger Movements. in Proceedings of the 2014 First International Conference on Systems Informatics, Modelling and Simulation. pp. 53-57.

[7] J. M. Romano, K. Hsiao, G. Niemeyer, S. Chitta and K. J. Kuchenbecker. 2011. Human-inspired robotic grasp control with tactile sensing. Robotics, IEEE Transactions on. 27: 1067-1079.

[8] N. Wettels, A. R. Parnandi, J.-H. Moon, G. E. Loeb, and G. Sukhatme. 2009. Grip control using biomimetic tactile sensing systems. Mechatronics, IEEE/ASME Transactions on. 14: 718-723.

[9] T. Takaki and T. Omata. 2011. High-performance anthropomorphic robot hand with grasping-force-magnification mechanism. Mechatronics, IEEE/ASME Transactions on. 16: 583-591.

[10] G. Sen Gupta, S. C. Mukhopadhyay, C. H. Messom, and S. N. Demidenko. 2006. Master–slave control of a teleoperated anthropomorphic robotic arm with gripping force sensing. Instrumentation and Measurement, IEEE Transactions on. 55: 2136-2145.

[11] Y. Lin, S. Ren, M. Clevenger, and Y. Sun. 2012. Learning grasping force from demonstration. in Robotics and Automation (ICRA), 2012 IEEE International Conference on, 2012, pp. 1526-1531.

[12] P. Payeur, C. Pasca, A.-M. Cretu and E. M. Petriu. 2005. Intelligent haptic sensor system for robotic manipulation. Instrumentation and Measurement, IEEE Transactions on. 54: 1583-1592.

[13] J. Becedas, I. Payo, and V. Feliu. 2011. Two-flexible-fingers gripper force feedback control system for its application as end effector on a 6-DOF manipulator. Robotics, IEEE Transactions on. 27: 599-615.

[14] V. Lippiello, F. Ruggiero, B. Siciliano, and L. Villani. 2013. Visual grasp planning for unknown objects using a multifingered robotic hand. Mechatronics, IEEE/ASME Transactions on. 18: 1050-1059.

[15] Tekscan. (2015, 15th July, 2015). Force Sensors for Design.Available:https://www.tekscan.com/flexiforce-e-book-force-sensors-design-download

[16] R. SCORBOT-ER. 4U User Manual Catalog# 100343 Rev. ed: B.

[17] R. Kumar, S. Kumar, S. Lal and P. Chand. 2014. Object detection and recognition for a pick and place Robot. in Computer Science and Engineering (APWC on CSE), 2014 Asia-Pacific World Congress on. pp. 1-7.

[18] Mathworks. 2015, 21st August. Polynomial curve fitting.Available:http://au.mathworks.com/help/matlab/ref/polyfit.html.

[19] W. Gautschi. 1962. On inverses of Vandermonde and confluent Vandermonde matrices. Numerische Mathematik. 4: 117-123.